韓國精密工學會 2003 年度 春季學術大會論文集 pp.300-304

Experimental verification of shear and frictional characteristics in end milling

Y. M. Lee*(Mechanical Eng. Dept., KNU), S. H. Yang(Mechanical. Eng. Dept., KNU),
M. Chen (Mechanical Eng. Dept., SJTU, China), S. I. Jang (Mech. Eng. Dept. Grad. School, KNU)

엔드밀링시 전단 및 마찰 특성의 실험적 검증

이영문(경북대 기계공학부), 양승한(경북대 기계공학부),
첸밍(중국, 상해교통대 기계공학부), 장승일(경북대 대학원 기계공학과)

ABSTRACT

As a new approach to analyze shear behaviors in the shear plane and chip-tool friction behaviors in the chip-tool contact region during an end milling process, this paper introduces a method to transform an end milling process to an equivalent oblique cutting process. In this approach, varying undeformed chip thicknesses and cutting forces in the up-and down-end milling process are replaced with the equivalent ones of oblique cutting. Accordingly, in the current paper, the shear and friction characteristics of end milling operations, up- and down-end milling, have been analyzed based on the equivalent oblique cutting models. Two series of cutting tests, up- and down-end milling tests and the equivalent oblique cutting tests to that, have been carried out to verify the validity of the analyses. And using the results of cutting tests the cutting characteristics of the up- and down-end milling processes have been thoroughly investigated.

Key Words : Shear, Chip-tool friction, Specific cutting energy, Up-end milling, Down-end milling, Equivalent oblique cutting

1. Introduction

Intermittent cutting process is performed by a rotating cutter while the workpiece is clamped onto a table and feed action is obtained by moving the table. In some cases the workpiece remains stationary, and the cutter is fed to the work. The undeformed chip thickness and cutting force components vary periodically with the cutter rotation during the cutting process.

Martellotti[1,2] was the first to establish the geometric relationships between the tool path and the cutting variables in the intermittent cutting process of milling.

Tlusty and Macneil[3] presented a mechanistic model for the prediction of cutting forces in up-end milling by multiplying an undeformed chip area by specific cutting forces, and verified the validity of the model by comparing computed cutting forces with the measured ones.

Zheng et al.[4] presented an angle domain analytical model for the prediction of cutting forces and an explicit expression of cutting force waveforms in an end milling operation with a helical multi-flute cutter.

Many other researchers[5~6] have also added their efforts to a fundamental understanding of intermittent cutting processes. However no analysis of the shear and friction processes in intermittent cutting has yet been attempted and there is no general standard to assess these processes.

Recently, Lee et al.[7~8] have proposed a model to simulate the shear and friction processes of an up- and down-end milling. But no effort has been exerted to verify the validity of the proposed model.

Accordingly, in the current paper, the shear and friction characteristics of end milling operations, up- and down-end milling, have been analyzed based on the equivalent oblique cutting models. And two series of cutting tests,

up- and down-end milling tests and the equivalent oblique cutting tests to those, have been carried out to verify the validity of the analyses. Using the results of cutting tests the cutting characteristics of the up- and down-end milling processes have been thoroughly investigated.

2. Equivalent oblique cutting model to intermittent cutting processes

2.1 End milling model

Figure 1 shows a cutting model, including a two-tooth cutter, of up- and down-end milling process along with the geometrical relations between tool and workpiece.

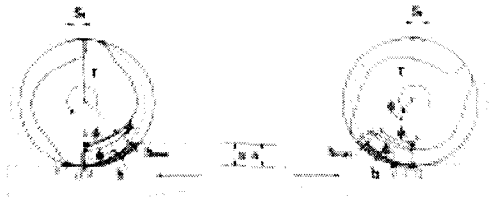

(a) (b)

Fig.1 Schematics of (a) up- (b) down-end milling process.

As seen in Fig.1 (a), the undeformed chip thickness, h in up-end milling is initially very small, reaches a maximum, and then decreases rapidly. In down-end milling as seen in Fig.1 (b), h increases rapidly at first and reaches a maximum, and then decreases gradually. The maximum undeformed chip thickness, h_{max} is as in Eq.(1).

$$h_{\max} = r - \sqrt{(r-a)^2 + \left\{\sqrt{r^2-(r-a)^2} - s_t\right\}^2} \qquad (1)$$

ϕ_1 is the rotation angle from the base position O when h reaches a maximum, and ϕ_2 is the rotation angle when the cutting edge escapes from the workpiece. ϕ_1 and ϕ_2 can be expressed as in Eq.(2) and (3).

$$\phi_1 = \cos^{-1}\left(\frac{r-a}{r-h_{\max}}\right) \qquad (2)$$

$$\phi_2 = \cos^{-1}\left(1-\frac{a}{r}\right) \qquad (3)$$

2.2 Equivalent oblique cutting model to an end milling

To establish an equivalent oblique cutting system equal to an end milling process, the cutting and tool geometrical variables must be matched. Oblique cutting is the simplest type of three-dimensional cutting processes achieved by a straight cutting edge that is inclined to the coordinate axis perpendicular to cutting velocity vector.

Figure 2 (a) shows cutting models of up- and down-end milling, respectively. Fig. 2 (b) shows unfolded undeformed chips along the workpiece movement direction of up- and down-end milling.

2.2.1 Equivalent oblique cutting angles to an end milling

The velocity rake angle, a_v in oblique cutting is the angle measured from a normal to the finished surface in a plane containing the cutting velocity vector.

Therefore, the radial rake angle, a_r in end milling equals the velocity rake angle, a_v in oblique cutting[9].

In the spread end milling model, the cutting edges meet the z axis with a helix angle, β which corresponds to the inclination angle, i in oblique cutting.

The normal rake angle, a_n in equivalent oblique cutting can be determined by Eq.(4).

$$\tan\alpha_n = \cos i \tan\alpha_v = \cos\beta \tan\alpha_r \qquad (4)$$

2.2.2 Equivalent oblique cutting conditions to an end milling

If constant intervals are assumed between consecutive cuttings in the spread end milling model, total unfolded length, L and average undeformed chip thickness, h_{av} can be determined. The axial depth of cut, b and cutting velocity, V in an end milling equal to the width of cut, b and cutting velocity, V in equivalent oblique cutting, respectively.

The average undeformed chip thickness, h_{av} is determined on the basis of the same volume of chips produced in an end milling and the equivalent oblique cutting process, as in Eq.(5).

$$h_{av} = a\, S_t\, Z \,/\, \pi\, d \qquad (5)$$

Where d is the tool diameter, z is the number of teeth, S_t is the feed per tooth, and a is the radial depth of the cut in the end milling.

Accordingly, the intermittent cutting process can be reduced to an equivalent continuous oblique cutting process with a constant undeformed chip thickness, h_{av}.

Figure 2 (c) shows the equivalent oblique cutting system equivalent to up- and down-end milling.

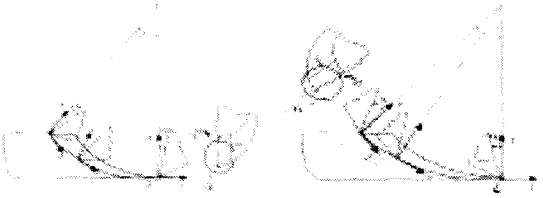

(a-1) (a-2)

(a) Cutting model of (a-1) up- and (a-2) down-end milling

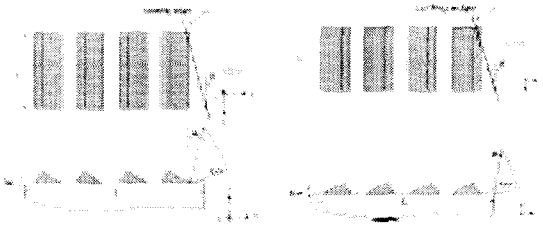

(a-1) (a-2)

(b) Spread (a-1) up- and (a-2) down-end milling model

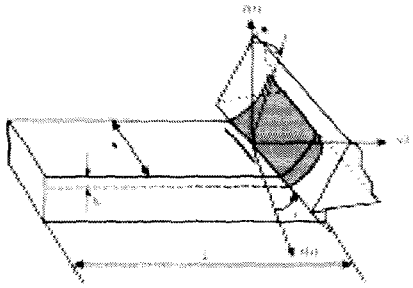

(c) Equivalent oblique cutting model

Fig. 2 Transformation end milling to equivalent oblique cutting model

3. Cutting experiments

Tungsten carbide two-tooth end-mills of 8mm diameter with 6° radial rake angle and 10° and 20° helix angles were used in the end milling tests. The equivalent oblique cutting tests were carried out on a lathe by cutting tube-like workpieces as seen in Fig. 3. Tools with 10° and 20° inclination angles were used.

Fig. 3 shows the tool and workpiece sets in the cutting tests i.e., an end milling and equivalent oblique cutting tests. To identify cutting conditions of the two processes, the undeformed chip thickness in the equivalent oblique cutting were determined using Eq.(5).

Table 1 shows the cutting tools and cutting test conditions of intermittent cutting and equivalent oblique cutting.

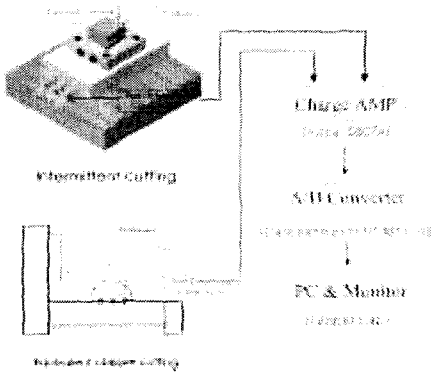

Fig.3 Schematic diagram for cutting tests.

The three cutting force components in end milling and equivalent oblique cutting were measured using a piezo-type tool dynamometer. Chips were also collected in end milling and equivalent oblique cutting tests for subsequent examination of their shape.

Table 1 Cutting conditions

End milling	
Work material	SM45C
Radial depth of cut, a (mm)	3
Axial depth of cut, b (mm)	2
Cutting velocity, V (m/min)	10.2, 15.9, 22.5
Radial rake angle, α_r (deg.)	6
Helix angle, β (deg.)	20
Number of teeth, Z	2
Feed per tooth, S_t (mm) 0.2051,0.2303,0.2428,0.2554,0.2805	
Equivalent Oblique cutting	
Work material	SM45C
Width of cut, b (mm)	2
Cutting velocity, V (m/min)	10.2, 15.9, 22.5
Velocity rake angle, α_v (deg.)	6
Inclination angle, i (deg.)	20
undeformed chip thickness, t (mm/rev) 0.049,0.055,0.058,0.061,0.067	

4. Results and discussions

4.1 Tangential and radial cutting forces

It is important to estimate the tangential(F_t) and radial(F_r) cutting forces for simulating the shear and friction processes of an end milling process.

The tangential(F_t) and radial(F_r) cutting forces can be estimated by multiplying the undeformed chip area by the specific cutting forces.

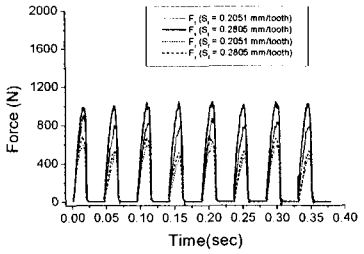

(a)

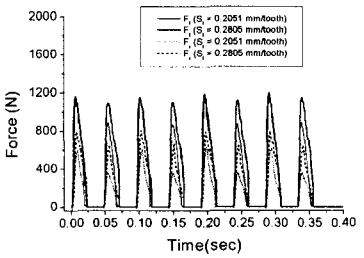

(b)

Fig.4-1 Tangential and radial cutting forces F_t and F_r (a) up- and (b) down-end milling for V = 15.9m/min.

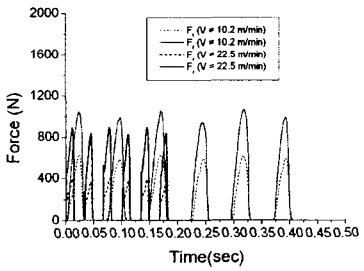

(a)

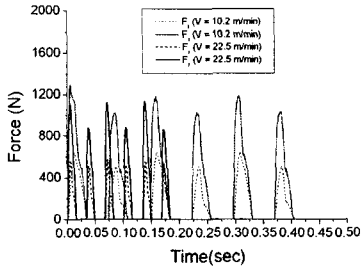

(b)

Fig.4-2 Tangential and radial cutting forces F_t and F_r (a) up- and (b) down-end milling for S_t = 0.2302 mm/tooth.

Figure 4-1 shows the tangential and radial cutting forces in up- and down-end milling process with the lowest(0.2051mm/tooth) and largest(0.2805mm/tooth) feed per tooth used in the experiments under the same cutting velocity of 15.9m/min. The tangential and radial cutting forces as seen in the figures increase as the feed per tooth increases.

Figure 4-2 shows the tangential and radial cutting forces in up- and down-end milling process with the lowest(10.2 m/min) and largest(22.5 m/min) cutting velocity used in the experiments under the same feed per tooth of 0.2302mm. As seen in figures, as the cutting velocity increases the tangential and radial cutting forces decrease.

4.2 Experimental verification of proposed equivalent oblique cutting model

4.2.1 Cutting forces in end milling based on equivalent oblique cutting model and oblique cutting

In an end milling model, the tangential(F_t), the radial(F_r), and the axial(F_z) cutting forces correspond to the main(F_y), the feed(F_z), and the thrust(F_x) cutting forces in the oblique cutting model, respectively.

Figures 5-1 and 5-2 show the cutting forces in end milling based on equivalent oblique cutting model and the oblique cutting tests along with the equivalent undeformed chip thicknesses[Fig. 5-1] and cutting velocities[Fig. 5-2].

There was no significant difference between the two sets of cutting forces as seen in the Figures.

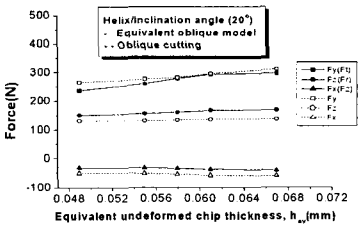

(a)

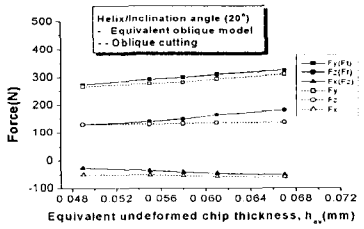

(b)

Fig.5-1 Cutting forces in equivalent oblique model to (a) up- and (b) down-end milling and oblique cutting for V = 15.9m/min.

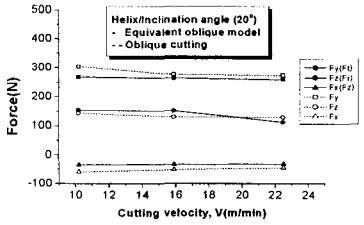

(a)

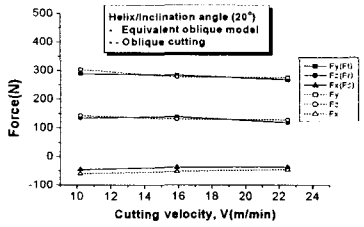

(b)

Fig.5-2 Cutting forces in equivalent oblique model to (a) up- and (b) down-end milling and oblique cutting for S_t = 0.2302mm/tooth.

4.2.2 Comparison of shear and friction characteristics in end milling with those in oblique cutting

Tables 2-1 and 2-2 show the friction and shear characteristic factors in end milling and the oblique cutting under the given cutting conditions seen in Table 1. The factors can be calculated by substituting the replaced cutting forces into the equivalent oblique cutting model.

Table 2-1 shows the shear and friction characteristic factors in up- and down-end milling and the oblique cutting under the same cutting velocity of 15.9m/min.

As seen in Table 2-1 (a) the friction forces and specific friction energies consumed in the up-end milling process were somewhat larger than those consumed in the oblique cutting. While the shear forces and specific shear energies were vice versa.

In down-end milling as seen in Table 2-1 (b), the friction forces and the specific friction energies consumed were somewhat larger than those of the oblique cutting. While the shear forces and specific shear energies were vice versa. 66 ~ 68% and 68 ~ 75% of the total energy was consumed in the shear processes in the up- and down-end milling, respectively. And 70 ~ 71% of the total energy was consumed in shear processes in the oblique cutting, respectively.

As such, these results coincided well with those of the continuous cutting[10,11]. The specific cutting energy decreases with an increase of undeformed thickness in end milling process. These experimental results can be explained based on "size effect" in cutting operations[10].

Table 2-2 shows the shear and friction characteristic factors in up- and down-end milling and the oblique cutting under the feed per tooth of 0.2302 mm. The specific cutting energy decreases with an increase of cutting velocity in end milling process. 70 ~ 72% and 75 ~ 73% of the total energy was consumed in the shear processes in the up- and down-end milling, respectively.

And 75 ~ 72% of the total energy was consumed in shear processes in the oblique cutting, respectively.

Table 2-1 Shear and friction characteristics in (a) up- (b) down-end milling with oblique cutting for V = 15.9m/min.

(a)

	Up-end milling	Oblique cutting
Friction Characteristics		
Friction force, F_c (N)	175.2 ~ 199.5	161.8 ~ 173.8
Specific friction energy, u_f (MPa)	812.7 ~ 717.8	783.3 ~ 682.1
Shear Characteristics		
Shear force, F_s (N)	150.3 ~ 197.1	189.9 ~ 230.8
Specific shear energy, u_s (MPa)	1600.6 ~ 1548.5	1957.7 ~ 1736.8
Cutting Characteristics		
Specific cutting energy, u (MPa)	2413.3 ~ 2266.3	2711.8 ~ 2315.1
u_f/u	0.34 ~ 0.32	0.29 ~ 0.30
u_s/u	0.66 ~ 0.68	0.71 ~ 0.70

(b)

	Down-end milling	Oblique cutting
Friction Characteristics		
Friction force, F_c (N)	155.7 ~ 221.8	161.8 ~ 173.8
Specific friction energy, u_f (MPa)	685.22 ~ 768.5	783.3 ~ 682.1
Shear Characteristics		
Shear force, F_s (N)	207.5 ~ 221.2	189.9 ~ 230.8
Specific shear energy, u_s (MPa)	2108.8 ~ 1639.9	1957.7 ~ 1736.8
Cutting Characteristics		
Specific cutting energy, u (MPa)	2794.0 ~ 2408.5	2711.8 ~ 2315.1
u_f/u	0.23 ~ 0.31	0.29 ~ 0.30
u_s/u	0.75 ~ 0.68	0.71 ~ 0.70

Table 2-2 Shear and friction characteristics in (a) up- (b) down-end milling with oblique cutting for St = 0.2302mm/tooth.

(a)

	Up-end milling	Oblique cutting
Friction Characteristics		
Friction force, F_c (N)	188.7 ~ 149.4	179.6 ~ 163.4
Specific friction energy, u_f (MPa)	736.6 ~ 654.1	683.5 ~ 691.9
Shear Characteristics		
Shear force, F_s (N)	187.8 ~ 186.9	227.9 ~ 196.5
Specific shear energy, u_s (MPa)	1701.8 ~ 1711.2	2076.6 ~ 1803.9
Cutting Characteristics		
Specific cutting energy, u (MPa)	2438.4 ~ 2365.3	2760.1 ~ 2495.8
u_f/u	0.30 ~ 0.28	0.25 ~ 0.28
u_s/u	0.70 ~ 0.72	0.75 ~ 0.72

(b)

	Down-end milling	Oblique cutting
Friction Characteristics		
Friction force, F_c (N)	172.2 ~ 154.7	179.6 ~ 163.4
Specific friction energy, u_f (MPa)	657.3 ~ 644.3	683.5 ~ 691.9
Shear Characteristics		
Shear force, F_s (N)	216.0 ~ 195.3	227.9 ~ 196.5
Specific shear energy, u_s (MPa)	1964.4 ~ 1784.5	2076.6 ~ 1803.9
Cutting Characteristics		
Specific cutting energy, u (MPa)	2621.7 ~ 2428.8	2760.1 ~ 2495.8
u_f/u	0.25 ~ 0.27	0.25 ~ 0.28
u_s/u	0.75 ~ 0.73	0.75 ~ 0.72

5. CONCLUSIONS

The equivalent oblique cutting model has been proposed to analyze the friction and shear processes of an end milling process and was verified through two sets of experiments. The experimental results show that the proposed model is suitable to analyze the shear and chip-tool frictional characteristics of down-end milling process.

And using the results of cutting tests the shear and friction characteristics of end milling operations, up- and down-end milling, have been analyzed based on the equivalent oblique cutting models

REFERENCES

1. Martellotti, M.E., "An Analysis of the Milling Process," Trans. ASME, Vol. 63, pp. 677-700, 1941.
2. Martellotti, M.E., "An Analysis of the Milling Process, part II - Down Milling," Trans. ASME, Vol. 67, pp. 233~250, 1945.
3. Tlusty, J. and Macneil, P., "Dynamics of Cutting Forces in End Milling," Annals of CIRP, Vol. 24, pp. 21-25, 1975.
4. Zheng, L., Liang, S. Y. and Melkote, S. N., "Angle Domain Analytical Model for End Milling Forces," ASME, J. Man. Sci. and Eng., Vol. 120, pp. 252-258, 1998.
5. Yang, M. Y. and Choi, J. G., " A Tool Deflection Compensation System for End Milling Accuracy Improvement," ASME, J. Man. Sci. and Eng., Vol. 120, pp. 222-229, 1998.
6. Altintas, Y., Engin, S., and Budak, E., " Analytical Stability Prediction and Design of Variable Pitch Cutters," ASME, J. Man. Sci. and Eng., Vol. 121, pp. 173-178, 1999.
7. Lee, Y. M., Yang, S., H., and Jang, S., I., "Shear and friction process in intermittent cutting," IJMPB, Vol.17, Nos.1 & 2, p.265-270, 2003.
8. Lee, Y. M. and Jang, S., I., "Shear and friction processes in down-end milling," Int. KSPE, Vol.4, No.4 -to be published, 2003.
9. Shaw, M. C., "Metal Cutting Principles," Oxford Univ. Press, New York, pp. 450-461, 1984.
10. Shaw, M. C., Cook, N. H., and Smith, P. A., 1951, "The Mechanics of Three dimensional Cutting Operations," Trans. ASME, Vol. 73, pp. 1055-1064.
11. Lee, Y. M., Choi, W. S., and Song, T. S., 2000, "Analysis of 3-D Cutting Process with Single Point Tool", . KSPE, Vol.1 No.1, pp.15-21.